Linear Co-ordinative Bonding at Oxygen: A Spectroscopic and Structural Study of Phosphine Oxide–Group 13 Lewis Acid Adducts†

Neil Burford,* Bruce W. Royan, Rupert E. v. H. Spence, T. Stanley Cameron, and Anthony Linden
Department of Chemistry, Dalhousie University, Halifax, Nova Scotia B3H 4J3, Canada
Robin D. Rogers
Department of Chemistry, Northern Illinois University, DeKalb, Illinois 60115, U.S.A.

A number of adducts composed of phosphine oxides and Group 13 Lewis acids $R_3PO{\cdot}EX_3$ (R = Ph, NMe_2, or PhO; E = B, Al, or Ga; X = F, Cl, or Br) have been spectroscopically characterised by multinuclear n.m.r. spectroscopy. Three isostructural derivatives have been structurally characterised by *X*-ray crystallography. Crystal data (all hexagonal, space group $R\bar{3}$, $Z = 6$): $Ph_3PO{\cdot}AlCl_3$, a = 13.663(2), c = 18.258(2) Å, R = 0.062; $Ph_3PO{\cdot}AlBr_3$, a = 14.021(6), c = 18.387(3) Å, R = 0.041; $Ph_3PO{\cdot}GaCl_3$, a = 13.753(6), c = 18.345(6) Å, R = 0.079. The structures show a uniquely linear or almost linear P–O–E backbone, which lies on the three-fold axis, in contrast to the bent structures observed for the corresponding BF_3 adducts and other related systems. Short Al–O bonds [X = Cl, 1.733(4); Br, 1.736(7) Å] are observed in both aluminium derivatives (E = Al). These compounds have narrow lines in the solution ^{27}Al n.m.r. spectra, indicative of a highly symmetric environment for the aluminium centre, and consistent with a linear geometry in solution. The results provide experimental evidence for axially symmetric dative bonding by oxygen, support the triple-bond model for the phosphine oxide unit, and imply the possibility of a delocalised π interaction over the P–O–E framework.

The electron-rich nature of nitrogen, oxygen, and fluorine allows for unusual structural flexibility in the two-co-ordinate environment with the ability to adopt a wide range of geometries. Consequently, the familiar electronic models of sp^3 hybridisation, for angles close to 109°, and sp^2 hybridisation, for angles close to 120°, are often inadequate to describe many of the observed structural arrangements. Similarly, terminal oxygen centres can also be difficult to categorise under either of these formulations. For example, the axial three-fold symmetry of a phosphoryl (R_3PO) group requires that the oxygen centre employ two degenerate p orbitals for π bonding to phosphorus and, therefore, the common valence-bond picture (**1**) (sp^2) is invalid. A more accurate model is a combination of resonance structures (**2**) and (**3**).[1] On this basis, the oxygen centre of a phosphoryl unit can be considered isolobal[2] with CO, NO^+, and CN^- and has the potential to adopt axial co-ordination. However, experimental evidence of such behaviour is limited.[3] Here we report a comparison of the spectroscopic properties of a number of derivatives of $R_3PO{\cdot}EX_3$ (R = Ph, NMe_2, or PhO; E = B, Al, or Ga; X = F, Cl, or Br) as well as structural studies of $Ph_3PO{\cdot}AlCl_3$, $Ph_3PO{\cdot}AlBr_3$, and $Ph_3PO{\cdot}GaCl_3$. The observations shed new light on the nature of the dative bond formed by oxygen, and provide experimental foundation for axial symmetry at oxygen.

Experimental

General Procedures.—The solvents CH_2Cl_2 and CCl_4 were dried over P_2O_5 and CaH_2 and stored over molecular sieves. N.m.r. spectra were recorded on a Nicolet NT-360 spectrometer in CH_2Cl_2. Chemical shifts are reported in p.p.m. relative to external standards {85% H_3PO_4 for ^{31}P, $Et_2O{\cdot}BF_3$ for ^{11}B, $[Al(H_2O)_6]^{3+}$ for ^{27}Al, and $[Ga(H_2O)_6]^{3+}$ for ^{71}Ga}, and relative to the internal CH_2Cl_2 signal for ^{13}C. Melting/decomposition points (Table 1) were recorded on a Fisher-Johns apparatus and are uncorrected. Glass equipment was flame dried before use. Reactions involved mixing a CH_2Cl_2 solution of a phosphine oxide with a solution or suspension of a Lewis acid in an evacuated (10^{-3} Torr, *ca.* 0.133 Pa) dual-compartment vessel. In the case of BCl_3 and BF_3, the gas was bubbled through the solution of phosphine oxide under an atmosphere of argon. Except for $(PhO)_3PO{\cdot}AlCl_3$ (reaction mixture, approximately 0.5 mol dm^{-3}), the compounds were isolated as solids, and where possible crystalline samples were prepared. N.m.r. spectra were obtained on samples (10-mm flame-sealed Pyrex tubes) prepared at an approximate concentration of 0.018 mol dm^{-3} in CH_2Cl_2. For the ^{71}Ga n.m.r. spectrum of $Ph_3PO{\cdot}GaCl_3$ the concentration was 0.18 mol dm^{-3}. The n.m.r. data are in Table 1, together with data for related compounds.

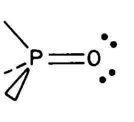

(1)

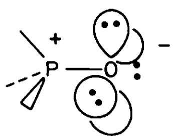

(2)

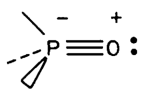

(3)

X-Ray Diffraction Analyses.—Crystals were obtained from solution (CH_2Cl_2) by slow removal of solvent ($Ph_3PO{\cdot}AlCl_3$ and $Ph_3PO{\cdot}GaCl_3$) and from a saturated solution (CH_2Cl_2–CCl_4, 1:1) on standing at room temperature ($Ph_3PO{\cdot}AlBr_3$). Transparent, block-shaped crystals were selected in a dry-box and mounted in Pyrex capillaries [$Ph_3PO{\cdot}AlCl_3$ (crystal fragments) and $Ph_3PO{\cdot}AlBr_3$ under N_2 and $Ph_3PO{\cdot}GaCl_3$ under Ar]. Enraf-Nonius CAD-4 diffractometers were used to measure the unit-cell dimensions and to collect the data. The crystal data and data collection details are listed in Table 2. The unit-cell constants were obtained by least-squares analysis of

---

† *Supplementary data available:* see Instructions for Authors, *J. Chem. Soc., Dalton Trans.*, 1990, Issue 1, pp. xix—xxii.

Table 1. N.m.r. data and melting points for derivatives of $R_3PO{\cdot}EX_3$ and related compounds; J_{CP} values and linewidths (Hz) are given in parentheses

	^{13}C						
Compound	*ipso*	*ortho*	*meta*	*para*	^{31}P	$^{27}Al/^{71}Ga/^{11}B$	M.p. (°C)
$Ph_3PO{\cdot}BF_3$	124.6	132.9	129.1	134.2	43.6	−0.9	229
	(112.1)	(11.4)	(13.4)	(1.9)		($\Delta\nu_{\frac{1}{2}}$ = 12.5)	
$Ph_3PO{\cdot}BCl_3$	122.9	133.5	129.3	134.8	46.7	6.2	191—194
	(110.4)	(11.8)	(13.7)			($\Delta\nu_{\frac{1}{2}}$ = 3.5)	
$Ph_3PO{\cdot}AlCl_3$	124.6	132.6	129.4	134.6	44.9	90	168—170
	(112.1)	(11.6)	(13.8)			($\Delta\nu_{\frac{1}{2}}$ = 40)	
$Ph_3PO{\cdot}AlBr_3$	124.1	132.8	129.5	134.8	45.7	79	157—160
	(109.8)	(11.8)	(13.6)			($\Delta\nu_{\frac{1}{2}}$ = 31)	
$Ph_3PO{\cdot}GaCl_3$	125.2	132.8	129.3	134.4	45.9	230	146—147
	(109.3)	(11.4)	(13.2)			($\Delta\nu_{\frac{1}{2}}$ = 5 100)	
Ph_3POH^{+} [a]	120.0	131.1	129.0	132.8	57.2		
(H_2SO_4)	(107.4)	(9.8)	(12.2)				
Ph_3PO [a]	132.8	132.1	128.5	131.8	29.3		
	(103.5)	(9.8)	(17.7)	(2.4)			
$(PhO)_3PO{\cdot}AlCl_3$	149.0	119.7	130.6	127.6	−23.4	90	
	($^2J_{CP}$ 8.4)	($^3J_{CP}$ 3.2)				($\Delta\nu_{\frac{1}{2}}$ = 220)	
$(PhO)_3PO$	150.5	120.1	129.9	125.6	−17.3 [b]		
	($^2J_{CP}$ 6.4)	($^3J_{CP}$ 3.4)			−18		
					−18.6		
$(Me_2N)_3PO{\cdot}AlCl_3$	36.4				24.4	88	138—141
						($\Delta\nu_{\frac{1}{2}}$ = 18)	
$(Me_2N)_3PO$					22.0—25.6 [b]		

[a] Values taken from ref. 10. [b] Values taken from M. M. Cruthfield, C. H. Dungan, J. H. Letcher, V. Mark, and J. R. Van Wazer, *Top. Phosphorus Chem.*, 1967, **5**.

Table 2. Crystal data collection and refinement parameters [a]

Compound	$Ph_3PO{\cdot}AlCl_3$ [b]	$Ph_3PO{\cdot}AlBr_3$	$Ph_3PO{\cdot}GaCl_3$
Formula	$C_{18}H_{15}AlCl_3OP$	$C_{18}H_{15}AlBr_3OP$	$C_{18}H_{15}Cl_3GaOP$
M	411.63	544.98	454.37
Lattice reflections (25), θ/°	15—17	>15	>20
Temperature/°C	−60	20	20
a/Å	13.663(2)	14.021(6)	13.753(6)
c/Å	18.258(2)	18.387(3)	18.345(6)
U/Å^3	2 951.8	3 130.4	3 005.0
F(000)	1 260	1 584	1 692
D_c/Mg m^{-3}	1.389	1.734	1.506
Crystal size/mm	0.15 × 0.25 × 0.35	0.18 × 0.25 × 0.30	0.13 × 0.20 × 0.33
λ(Mo-K_α)/Å	0.709 26	0.710 73	0.710 73
μ/cm^{-1}	5.93	62.61	19.26
Absorption correction			
max.	1.133	1.00	1.00
min.	0.724	0.85	0.85
Scan range/°	4 < 2θ < 50	2 < 2θ < 50	2 < 2θ < 50
Range of *h*, *k*, *l*	±16, +16, +21 ($-h + k + l = 3n$ only)	±16, +16, +21	+16, ±16, +21 ($h + k + l = 3n + 1$ not collected)
Standard reflections	−4 −3 11, −7 −4 11, −3 −7 11	600, 060, 009	600, 060, 009
Variation/%	±2	±1	±2
Reflections measured	1 691	3 675	1 900
Unique observed reflections	642 [$I > 2\sigma(I)$]	692 [$I > 2.5\sigma(I)$]	781 [$I > 2.5\sigma(I)$]
Parameters refined	78	82	82
$w = k/[\sigma^2(F_o) + gF_o^2]$	k = 1.8743 g = 0.000 541	1 0.0002	1 0.000 12
R	0.0622	0.041	0.079
R′	0.0599	0.042	0.080
Goodness of fit	2.37	1.22	3.95
Largest feature in final difference map/e Å^{-3}	0.33	1.0	1.0

[a] Details in common: crystal class, hexagonal; space group, $R\bar{3}$; $Z = 6$; scan type, ω—2θ; $R = \Sigma(||F_o| - |F_c||)/\Sigma F_o$; $R' = [\Sigma(w(||F_o| - |F_c||)^2/\Sigma(w|F_o|)^2]^{\frac{1}{2}}$; goodness of fit = $[\Sigma(w(||F_o| - |F_c||)^2/(N_o - N_v)]^{\frac{1}{2}}$ where N_o = number of reflections and N_v = number of parameters. [b] At 20 °C, a = 13.716(2) and c = 18.369(2) Å.

the diffractometer setting angles of 25 well centred reflections. The space groups were determined from systematic absences, consideration of unit-cell volumes and molecular geometry, and were confirmed upon refinement of the structures.

Solution and refinement. Lorentz and polarisation corrections were applied. Scattering factors for neutral atoms were obtained from ref. 4 and corrected for the real part of the anomalous dispersion. The structures were solved by direct methods (SHELX 76[5] for $Ph_3PO{\cdot}AlCl_3$, SHELXS[6] for $Ph_3PO{\cdot}AlBr_3$ and $Ph_3PO{\cdot}GaCl_3$) and refined (SHELX 76) by a full-matrix least-squares procedure using anisotropic thermal parameters for all non-hydrogen atoms.

$Ph_3PO{\cdot}AlCl_3$. Absorption corrections were applied (empirical, DIFABS).[7] The hydrogen atoms were placed in geometrically calculated positions 1.08 Å from each carbon atom and constrained to ride on that atom. Individual isotropic thermal parameters were refined for the hydrogen atoms.

$Ph_3PO{\cdot}AlBr_3$. Absorption corrections were applied (empirical, ψ scan). Disorder was observed in the $AlBr_3$ portion of the molecule. Two bromine atom positions were resolvable and were refined in alternate least-squares cycles each with 50% occupancy. Although the thermal parameters of the oxygen atom imply an elongation perpendicular to the three-fold axis, it was not possible to resolve any disorder. The hydrogen atoms were placed in calculated positions 0.95 Å from each carbon atom and constrained to ride on that atom with B fixed at 5.5 Å^2.

$Ph_3PO{\cdot}GaCl_3$. Absorption corrections were applied (empirical, ψ scan). The disorder observed for the chlorine atom positions corresponds with that observed in $Ph_3PO{\cdot}AlBr_3$ and these atoms were refined in alternate least-squares cycles each with 50% occupancy. The problems associated with the oxygen atom position are more pronounced in this compound. The thermal ellipsoid is severely elongated perpendicular to the three-fold axis, which suggests disorder of the oxygen atom. This could be indicative of a bent geometry at oxygen. Under reduced symmetry of $P\bar{1}$, the approximate angles at oxygen ranged from 162 to 170°. The hydrogen atoms were placed in geometrically calculated positions, 0.95 Å from each carbon atom and constrained to ride on that atom with B fixed at 5.5 Å^2.

Final fractional co-ordinates for $Ph_3PO{\cdot}AlCl_3$, $Ph_3PO{\cdot}AlBr_3$, and $Ph_3PO{\cdot}GaCl_3$ are listed in Tables 3, 4, and 5, respectively, bond lengths and angles in Table 6. Views of the molecular units are shown in Figures 1, 2, and 3, respectively, a representative unit-cell packing diagram ($Ph_3PO{\cdot}AlBr_3$) in Figure 4.[8]

Additional material available from the Cambridge Crystallographic Data Centre comprises H-atom co-ordinates and thermal parameters.

Results and Discussion

A series of closely related adducts of the form $R_3PO{\cdot}EX_3$ have been studied by n.m.r. spectroscopy in CH_2Cl_2 solution and by X-ray crystallography. In general, the results essentially confirm and complement the conclusions derived from i.r. spectroscopic data for these derivatives and related complexes.[9] However, novel features are observed which further contribute to our understanding of the electronic structure at oxygen. Derivatives have been selected to examine the influence of specific molecular components on the spectroscopic and structural features of the adducts. The compounds under investigation are listed in Table 1, together with n.m.r. data, melting points, and comparative data for related compounds. Heating of the n.m.r. samples to 80 °C for 15 h had no effect on the spectra, except in the case of $Ph_3PO{\cdot}AlBr_3$, as described below.

Spectroscopic Data.—The n.m.r. spectral data for all derivatives under investigation are very similar. The ^{31}P chemical shifts of the Ph_3PO adducts are deshielded from the free base to a degree which is essentially independent of the Group 13 acid, although the effect is more pronounced for the conjugate acid Ph_3POH^+.[10] The observations are indicative of disruption of the PO π interaction as a result of adduct bond formation, in agreement with i.r. data.[9] Consequently, the phosphonium character of the phosphorus centre is enhanced in the adduct with respect to the free base. When R = NMe_2 or PhO the phosphorus centre is less sensitive to change at the oxygen centre. The difference in ^{31}P chemical shift for $(Me_2N)_3PO$ and $(Me_2N)_3PO{\cdot}AlCl_3$ is small, and a slight shielding is observed at phosphorus of $(PhO)_3PO{\cdot}AlCl_3$ with respect to $(PhO)_3PO$. These results are perhaps demonstrative of an electronic buffering of the phosphorus centre by means of π donation from the nitrogen centres of NMe_2 and the oxygen centres of PhO, respectively.

The electronic adjustments associated with adduct formation are also transmitted to the carbon centres of the phenyl groups of Ph_3PO derivatives. An upfield shift is observed for the *ipso* positions and the *para* positions show a downfield shift, relative to those positions of Ph_3PO. In addition, $^1J_{CP}$ is significantly larger for the adducts than for the free base. These features parallel those of the phosphorus ylides and their corresponding cations,[11] and confirm the phosphonium model[10] for the adducts. The effects can be rationalised in terms of simple resonance considerations and provide evidence for π interaction between the phenyl groups and the phosphorus centre. The ^{11}B n.m.r. chemical shift of $Ph_3PO{\cdot}BF_3$ (−0.9 p.p.m.) is slightly upfield from that of the free acid BF_3 (9.4—11.6 p.p.m.),[12] as reported for related adducts of BF_3.[12] A more substantial shielding is observed for the $Ph_3PO{\cdot}BCl_3$ adduct (6.2 p.p.m.), relative to BCl_3 (41.9—47.0 p.p.m.),[12] perhaps demonstrating a more dramatic electronic adjustment upon adduct formation for the stronger acid.

Narrow signals are observed in the ^{27}Al n.m.r. spectra of $Ph_3PO{\cdot}AlCl_3$ ($\Delta\nu_{\frac{1}{2}}$ = 40 Hz), $Ph_3PO{\cdot}AlBr_3$ ($\Delta\nu_{\frac{1}{2}}$ = 31 Hz), and $(Me_2N)_3PO{\cdot}AlCl_3$ ($\Delta\nu_{\frac{1}{2}}$ = 18 Hz), diagnostic of a highly symmetric environment for the aluminium centre in solution (*cf.* $AlCl_4^-$, $\Delta\nu_{\frac{1}{2}}$ = 3; $AlEt_3{\cdot}OEt_2$, $\Delta\nu_{\frac{1}{2}}$ = 1 160 Hz).[13] The data imply a pseudo-tetrahedral environment at aluminium by virtue of a linear P–O–Al backbone in solution, in agreement with the structures observed in the solid state (see below). The sharp line observed for $(Me_2N)_3PO{\cdot}AlCl_3$ ($\Delta\nu_{\frac{1}{2}}$ = 18 Hz) is consistent with the related solvate system $[Al\{OP(NMe_2)_3\}_4]^{3+}$ for which a coupling constant can be measured ($\Delta\nu_{\frac{1}{2}}$ = 3—5 Hz, $^2J_{AlP}$ = 30 Hz).[3,13a,14] However, the structural data available for complexes of $(Me_2N)_3PO$ show the familiar bent geometry at oxygen [V–O–P in $2(Me_2N)_3PO{\cdot}VOCl_2$ 154°;[15] see also Table 7] in the solid state. The broader signal observed for $(PhO)_3PO{\cdot}AlCl_3$ ($\Delta\nu_{\frac{1}{2}}$ = 220 Hz) is possibly a consequence of the increased flexibility of the phenoxy groups relative to the more restricted phenyl and dimethylamino groups, or competition for adduct formation at the two-co-ordinate oxygen and nitrogen centres, respectively.

In contrast to the oxide adducts of $AlCl_3$, the related chalcogenide adducts $Ph_3PS{\cdot}AlCl_3$ and $Ph_3PSe{\cdot}AlCl_3$ have bent structures in the solid state, and broad signals (300 Hz) are observed in the solution ^{27}Al n.m.r. spectra.[16] While ^{71}Ga n.m.r. signals are intrinsically broader (higher quadrupole moment) than the corresponding aluminium signals,[3,13b] it is difficult to correlate the very broad single line (5100 Hz) observed in the ^{71}Ga n.m.r. spectrum of $Ph_3PO{\cdot}GaCl_3$ with the solid state structure (see below).

Following heating of the $Ph_3PO{\cdot}AlBr_3$ sample, at 80 °C for 15 h, three ^{27}Al n.m.r. signals are observed at 90.2, 87.5, and 83.6 p.p.m., of similar integration. We assign these signals to $Ph_3PO{\cdot}AlCl_3$, $Ph_3PO{\cdot}AlCl_2Br$, and $Ph_3PO{\cdot}AlClBr_2$, respectively, by

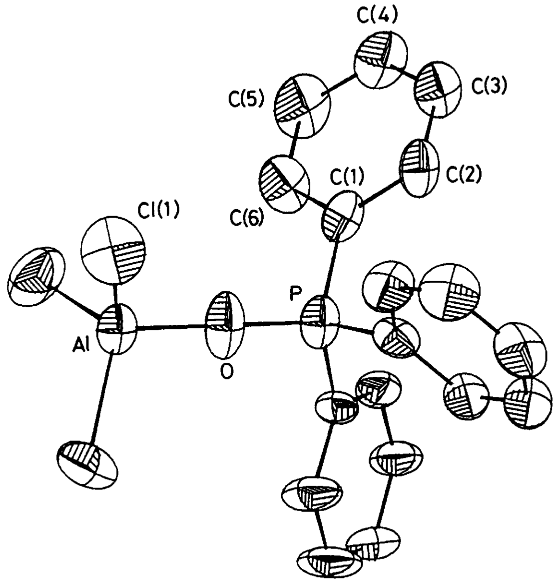

Figure 1. A view of $Ph_3PO{\cdot}AlCl_3$

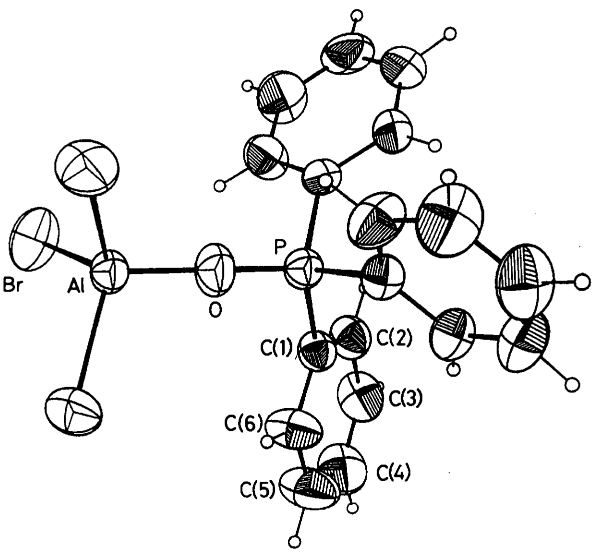

Figure 2. A view of $Ph_3PO{\cdot}AlBr_3$

Table 3. Final fractional co-ordinates for $Ph_3PO{\cdot}AlCl_3$

Atom	X/a	Y/b	Z/c	$U_{eq.}$*
P	0.0	0.0	0.174 3(1)	0.0436
O	0.0	0.0	0.257 5(3)	0.0619
Al	0.0	0.0	0.352 4(1)	0.0417
Cl	−0.168 6(1)	−0.101 2(1)	0.385 9(1)	0.0953
C(1)	−0.021 4(4)	−0.131 8(4)	0.140 6(3)	0.0421
C(2)	−0.099 1(5)	−0.190 0(5)	0.085 7(3)	0.0507
C(3)	−0.108 5(5)	−0.288 2(5)	0.057 3(3)	0.0562
C(4)	−0.040 4(5)	−0.327 2(5)	0.082 9(3)	0.0609
C(5)	0.036 3(6)	−0.271 4(5)	0.138 8(3)	0.0689
C(6)	0.044 6(5)	−0.173 9(5)	0.166 9(3)	0.0606

* $U_{eq.}$ is defined as one third of the trace of the orthogonalised U_{ij} tensor.

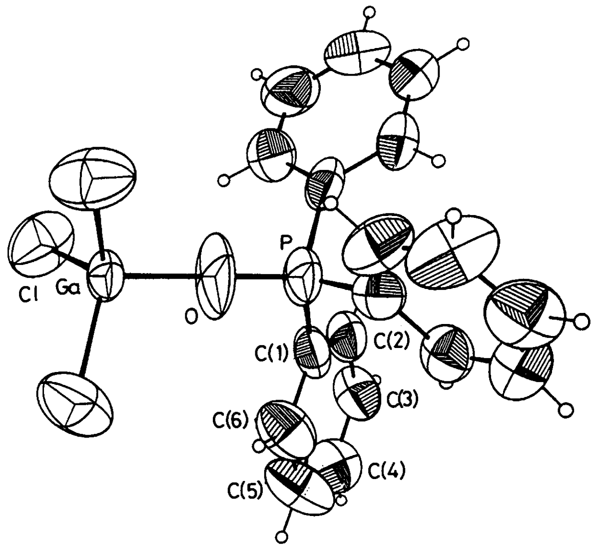

Figure 3. A view of $Ph_3PO{\cdot}GaCl_3$

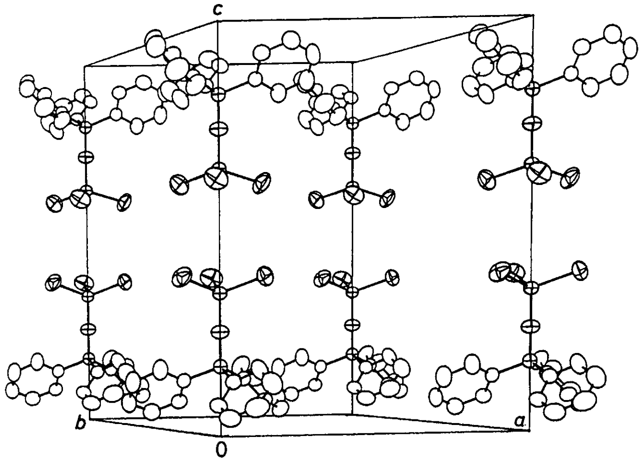

Figure 4. A view of the unit cell of $Ph_3PO{\cdot}AlBr_3$, which is representative of all three structures

Table 4. Final fractional co-ordinates for $Ph_3PO{\cdot}AlBr_3$

Atom	X/a	Y/b	Z/c	$B_{eq.}$ [a]
P	0.0	0.0	0.173 0(1)	2.73
O	0.0	0.0	0.255 3(3)	4.03
Al	0.0	0.0	0.349 7(2)	2.79
Br	−0.175 4(1)	−0.114 4(1)	0.390 1(1)	4.98
Br′ [b]	0.098 2(2)	0.178 5(1)	0.380 9(1)	5.45
C(1)	−0.024 1(5)	−0.130 1(4)	0.139 6(3)	2.81
C(2)	−0.099 2(5)	−0.185 2(5)	0.085 3(3)	3.53
C(3)	−0.113 1(6)	−0.283 6(6)	0.059 1(4)	4.33
C(4)	−0.050 3(7)	−0.323 8(5)	0.085 7(4)	5.05
C(5)	0.024 3(7)	−0.269 5(6)	0.139 5(6)	5.94
C(6)	0.037 0(5)	−0.173 6(5)	0.168 3(4)	4.45

[a] $B_{eq.} = \frac{4}{3}\,[(a^2)\beta11 + (b^2)\beta22 + (c^2)\beta33 + ab(\cos\ \beta)(\beta12) + ac(\cos\ \beta)(\beta13) + bc(\cos\ \alpha)(\beta23)]$. [b] Refined at 50% occupancy.

comparison with the data for $Ph_3PO{\cdot}AlCl_3$ and by analogy with the data for the series of corresponding mixed tetrahalogenoaluminate anions, $AlX_nY_m^-$ (X = Cl, Y = Br, $n = 4 - m$, $m = 4 - n$).[17] The apparent exchange process involving transfer of chlorine from the solvent is similar to that reported for related BF_3 adducts,[18] and in this case is probably a result of the strong thermodynamic preference for the Al–Cl bond.

Crystal Structures of $Ph_3PO{\cdot}AlCl_3$, $Ph_3PO{\cdot}AlBr_3$, *and* $Ph_3PO{\cdot}GaCl_3$.—The three compounds are isostructural in the

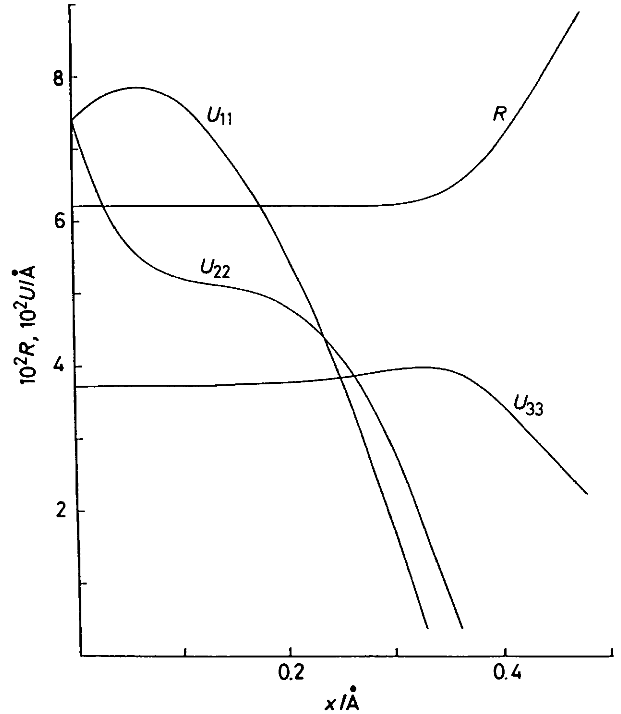

Figure 5. Variation of U_{ii} and R for $Ph_3PO{\cdot}AlCl_3$ with displacement of the x co-ordinate of the oxygen atom from the three-fold axis

Table 5. Final fractional co-ordinates for $Ph_3PO{\cdot}GaCl_3$. Footnotes as in Table 4

Atom	X/a	Y/b	Z/c	$B_{eq.}$[a]
P	0.0	0.0	0.175 0(2)	5.04
O	0.0	0.0	0.256 1(6)	9.74
Ga	0.0	0.0	0.355 2(1)	3.82
Cl	−0.163 5(5)	−0.122 2(5)	0.387 8(4)	7.48
Cl′[b]	0.092 7(7)	0.171 0(5)	0.384 9(3)	7.69
C(1)	−0.020 4(7)	−0.128 9(8)	0.141 7(4)	4.33
C(2)	−0.096 2(8)	−0.187 5(8)	0.086 1(4)	4.91
C(3)	0.105(1)	−0.284 8(8)	0.056 4(5)	5.59
C(4)	−0.038(1)	−0.325 9(9)	0.085 0(7)	6.32
C(5)	0.034(1)	−0.271(1)	0.139 1(7)	7.31
C(6)	0.043(1)	−0.173(1)	0.169 0(6)	5.99

Table 6. Bond lengths (Å) and angles (°) for $Ph_3PO{\cdot}EX_3$ (X = Cl or Br, E = Al or Ga)

	$Ph_3PO{\cdot}AlCl_3$	$Ph_3PO{\cdot}AlBr_3$	$Ph_3PO{\cdot}GaCl_3$
P–O	1.519(4)	1.513(7)	1.487(11)
O–E	1.733(4)	1.736(7)	1.818(10)
X–E	2.099(2)	2.287(2)	2.112(6)
X–E′		2.245(2)	2.111(6)
P–C(1)	1.784(5)	1.791(7)	1.761(11)
C(1)–C(2)	1.385(8)	1.374(8)	1.391(11)
C(2)–C(3)	1.384(8)	1.38(1)	1.394(17)
C(3)–C(4)	1.365(8)	1.35(1)	1.398(21)
C(4)–C(5)	1.387(9)	1.36(1)	1.338(16)
C(5)–C(6)	1.377(8)	1.37(1)	1.401(20)
C(1)–C(6)	1.376(7)	1.38(1)	1.390(19)
P–O–E	180	180	180
O–E–X	106.92(10)	108.95(8)	106.44(19)
O–E–X′		104.79(8)	104.97(17)
X–E–X^I	111.89(9)	109.99(8)	112.32(17)
X′–E–X'^I		113.72(7)	113.58(14)
O–P–C(1)	110.2(2)	110.1(2)	110.34(29)
C(1)–P–C(1^I)	108.8(2)	108.8(2)	108.58(30)
P–C(1)–C(2)	121.3(4)	121.6(6)	122.3(10)
P–C(1)–C(6)	119.4(4)	118.4(4)	120.0(7)
C(1)–C(2)–C(3)	120.0(6)	120.0(8)	121.4(12)
C(2)–C(3)–C(4)	119.9(6)	119.7(6)	119.0(9)
C(3)–C(4)–C(5)	120.9(6)	120.5(8)	120.4(13)
C(4)–C(5)–C(6)	118.7(6)	121.0(9)	120.7(15)
C(1)–C(6)–C(5)	121.3(6)	118.7(6)	120.8(10)
C(2)–C(1)–C(6)	119.2(5)	120.0(7)	117.6(11)

* Superscript I indicates atom related by $-y, x - y, z$.

space group $R\bar{3}$. The cell parameters for $Ph_3PO{\cdot}GaCl_3$ in space group $P\bar{1}$ have been previously reported.[19] Each structure consists of discrete molecules with no unusual intermolecular contacts. A linear geometry is observed with the P–O–E framework lying on the crystallographic three-fold axis of $R\bar{3}$. Despite the isostructural relationship, it was possible to resolve disorder in the EX_3 group for the $AlBr_3$ and $GaCl_3$ adducts. The halogen atoms of the $AlBr_3$ and $GaCl_3$ units have been modelled with two distinct positions, each with a 50% occupancy. The oxygen centre of $Ph_3PO{\cdot}GaCl_3$ exhibits a large degree of off-axis motion, indicative of a bent geometry at oxygen, however modelling of possible disorder has been unsuccessful. The linearity of the P–O–Al backbone in $Ph_3PO{\cdot}AlCl_3$ and $Ph_3PO{\cdot}AlBr_3$ is more reliable. While the thermal ellipsoids of the phosphorus, aluminium, and particularly the oxygen atom of $Ph_3PO{\cdot}AlCl_3$ produce somewhat oblate spheroids, with the minor axis along the three-fold axis, any disorder of the oxygen atom is barely detectable from the X-ray data. The difference Fourier synthesis shows a small peak (height 0.17 e) adjacent to the oxygen site in the direction of the x (y or i) axis. When the oxygen atom is displaced in the direction of this peak and its anisotropic thermal parameters allowed to refine, the R factor remains unchanged (four decimal places) over displacements ranging from 0 to 0.26 Å and rises rapidly with larger displacements. Thus R is not particularly sensitive to small displacements of the oxygen atom in the xy plane. A position of the oxygen atom at 0, 0, z with librations along x, y, and i and with a mean Al–O–P bond angle of 180° is one interpretation of these results.

However, as the oxygen atom is displaced along the x axis, U_{11} rises slightly from 0.074 $Å^2$ at zero displacement to a maximum of 0.0788 $Å^2$ at a displacement of 0.060 Å and then falls sharply, while U_{22} falls steeply from the initial value of 0.074 to reach a value of 0.0552 $Å^2$ at a displacement of 0.060 Å and then falls more slowly* until U_{11} equals U_{22} with a value of 0.042 $Å^2$ at a displacement of 0.23 Å, see Figure 5. Thus a second interpretation of these observations would be a libration of the oxygen atom along the x, y, and i directions with the centre of the libration displaced 0.06 Å from the three-fold axis. This would produce a minimum Al–O–P bond angle of 175.8°. The P–O–P backbone linearity of the related pyrophosphate anion has been a point of considerable discussion on a similar basis.[20] The bond lengths and angles of the Ph_3PO moiety in the three structures are essentially identical. The P–O bond lengths [EX_3 = $AlCl_3$, 1.519(4); $AlBr_3$, 1.513(7); $GaCl_3$, 1.49(1) Å] are significantly longer than in the isolated Ph_3PO molecule [1.483(2),[21a] 1.46(1) Å;[21b] see also Table 7], but are substantially shorter than a P–O single bond (*e.g.* 1.60 Å in P_4O_{10}).[22] The observed lengthening of the P–O bond in the adducts is

---

* Beyond a certain displacement, the values of U_{11}, U_{22}, and U_{33} all fall rapidly, which is presumed to be an attempt by the refinement to compensate for a loss of electron density at the true atomic location(s) of the oxygen atom. When the x co-ordinate of the oxygen atom is displaced from the three-fold axis by 0.26 Å (−0.02, 0, z) and x is allowed to refine the refinement converges at the position represented by the inflection in the U_{22} curve in Figure 5.

Table 7. Comparison of structural features for some phosphine oxide complexes and related compounds

Compound	P–O (Å)	P–O–M (°)	Ref.
Ph_3PO	1.483(2)		21*a*
$Ph_3PO{\cdot}BF_3$	1.522(3)	134.5(2)	33
$Ph_3PO{\cdot}AlCl_3$	1.519(4)	180	
$Ph_3PO{\cdot}AlBr_3$	1.513(7)	180	
$Ph_3PO{\cdot}AlO_3(SiPh)_7O_9$	1.508(4)	160.4(3)	25*e*
$Ph_3PO{\cdot}GaCl_3$	1.49(1)	180	
$Ph_3PO{\cdot}SeOCl_2$	1.520(8)	123.0(4)	*a*
	1.497(9)	142.5(4)	
		143.4(5)	
$(Ph_3PO)_2{\cdot}MnCl_2$	1.488(6)	156.0(4)	*b*
$[NpO_2(Ph_3PO)_2]^{2+}$	1.502(9)	159.1(4)	*c*
$[UO_2(Ph_3PO)_2]^{2+}$	1.505(9)	160.0(4)	*c*
$[NpO_2Cl_2(Ph_3PO)_2]$	1.50(1)	167(1)	*c*
	1.55(2)	153(1)	
$[\{ReCl_2(O)Me(Ph_3PO)\}_2O]$	1.524(4)	171.7(3)	*d*
cis-$[\{Sm(\eta\text{-}C_5Me_5)_2(Ph_3PO)\}_2(C_2H_2O_2)]$	1.501(10)	167.6(6)	*e*
	1.496(11)	168.8(7)	
trans-$[\{Sm(\eta\text{-}C_5Me_5)(Ph_3PO)\}_2(C_2H_2O_2)]$	1.514(7)	163.0(5)	*e*
	1.495(8)	158.7(5)	
$[TlCl(Br)I(Ph_3PO)_2]$	1.491(4)	149.0(2)	*f*
	1.485(4)	148.5(2)	
$[Cu_2(MeCHClCO_2)_4(Ph_3PO)_2]$	1.507(6)	146.7(4)	*g*
$[Cu_2(ClCH_2CH_2CO_2)_4(Ph_3PO)_2]$	1.477(3)	149.0(2)	*h*
$[Os(oep)(Ph_3PO)_2]$	1.483(8)	154.2(5)	*i*
$[La\{N(SiMe_3)_2\}_3(Ph_3PO)]$	1.52(2)	174.6(9)	*j*
$[La_2(O_2)\{N(SiMe_3)_2\}_4(Ph_3PO)_2]$	1.51(2)	172.6(14)	*j*
		138.5(14)	
$[Co(NO_3)_2(Ph_3PO)_2]$	1.48(1)	158.5(8)	*k*
$[SnCl_2Me_2(CH_2)_2\overline{PO{\cdot}SnClMe_2CH_2C}H_2]$	1.501(6)	113.4(3)	*l*
$Me_3PO{\cdot}SbCl_5$	1.56(4)	144.9(23)	32
$Cl_3PO{\cdot}SbCl_5$	1.47(2)	145(16)	32
$Cl_3PO{\cdot}NbCl_5$	1.45(2)	148.8(12)	32
$Cl_3PO{\cdot}MoCl_5$	1.459(7)	143.7(4)	31
$Cl_3PO{\cdot}MoNCl_3$	1.45(2)	151.6(9)	31
$Cl_3PO{\cdot}MoNCl_4(C_2Cl_5)$	1.426(9)	160.3(6)	*m*
$[Cl_3PO{\cdot}Mo(NO)Cl_3]_2$	1.439(5)	149.8(4)	*n*
$Cl_3PO{\cdot}WCl_4(C_{10}H_{18})$	1.456(12)	146.1(8)	*o*
$(Cl_3PO{\cdot}WNCl_3)_4$	1.393(5)	152.4(1)	*p*
	1.530(3)	146.9(1)	
	1.534(3)	146.6(1)	
	1.517(4)	157.9(3)	
$Cl_3PO{\cdot}ReCl_5$	1.45(1)	143.2(8)	*q*
$Cl_3PO{\cdot}ReNCl_4(C_2Cl_5)$	1.434(11)	158.6(6)	*r*
$Cl_3PO{\cdot}TiCl_4$	1.44(2)	151.8(13)	*s*
$[SnCl_5(Cl_3PO)]^-$	1.46(1)	147.3(6)	*t*
$Ph_3AsO{\cdot}BF_3$		125.7(2)	33
$2Ph_3AsO{\cdot}HgCl_2$		135.5	*u*
$Me_2SO{\cdot}BF_3$		119.2	*v*

[a] Y. Hermodsson, *Ark. Kemi*, 1969, **30**, 15. [b] K. Tomita, *Acta Crystallogr., Sect. C*, 1985, **41**, 1832. [c] N. W. Alcock, M. M. Roberts, and D. Brown, *J. Chem. Soc., Dalton Trans.*, 1982, 25. [d] J. K. Felixberger, J. G. Kuchler, E. Herdtweck, R. A. Paciello, and W. A. Hermann, *Angew. Chem., Int. Ed. Engl.*, 1988, **27**, 946. [e] W. J. Evans, J. W. Grate, and R. J. Doedens, *J. Am. Chem. Soc.*, 1985, **107**, 1671. [f] M. R. Bermjo, A. Fernandez, M. Gayoso, A. Castineiras, W. Hiller, and J. Strahle, *Polyhedron*, 1988, **7**, 2561. [g] B. Koren, P. Sivy, F. Valach, M. Melnik, and J. Jecny, *Acta Crystallogr., Sect. C*, 1988, **44**, 646. [h] P. Sharrock, M. Melnik, F. Belanger-Gariepy, and A. L. Beauchamp, *Can. J. Chem.*, 1985, **63**, 2564. [i] C-M. Che, T-F. Lai, W-C. Chung, W. P. Schaefer, and H. B. Gray, *Inorg. Chem.*, 1987, **26**, 3907; oep^{2-} = octaethylporphyrinate. [j] D. C. Bradley, J. S. Ghotra, F. A. Hart, M. B. Hursthouse, and P. R. Raithby, *J. Chem. Soc., Dalton Trans.*, 1977, 1166. [k] A. M. G. Dias Rodrigues, R. H. P. Francisco, and J. R. Lechat, *Cryst. Struct. Comm.*, 1982, **11**, 847. [l] M. Dargatz, H. Hartung, E. Kleinpeter, B. Rensch, D. Schollmeyer, and H. Weichmann, *J. Organomet. Chem.*, 1989, **361**, 43. [m] K. Dehnicke, U. Weiher, and D. Fenske, *Z. Anorg. Allg. Chem.*, 1979, **456**, 71. [n] K. Dehnicke, A. Liebelt, and F. Weller, *Z. Anorg. Allg. Chem.*, 1981, **474**, 83. [o] G. Uhl, E. Hey, G. Becker, F. Weller, and K. Dehnicke, *Z. Anorg. Allg. Chem.*, 1983, **497**, 213. [p] W. Musterle, J. Strahle, W. Liebelt, and K. Dehnicke, *Z. Naturforsch., Teil B*, 1979, **34**, 942. [q] P. Klingelhofer, U. Muller, H. G. Hauck, and K. Dehnicke, *Z. Naturforsch., Teil B*, 1984, **39**, 135. [r] U. Weiher, K. Dehnicke, and D. Fenske, *Z. Anorg. Allg. Chem.*, 1979, **457**, 115. [s] C. I. Branden and I. Lindqvist, *Acta Chem. Scand.*, 1960, **14**, 726. [t] A. J. Banister, J. A. Durrant, I. Rayment, and H. M. M. Shearer, *J. Chem. Soc., Dalton Trans.*, 1976, 928. [u] C. I. Branden, *Acta Chem. Scand.*, 1963, **17**, 1363. [v] I. Lindqvist, 'Inorganic Adduct Molecules of Oxo-compounds,' Springer, Berlin, 1963.

consistent with the low P–O stretching frequency observed in the i.r. spectra, compared with that of the free base.[9] The P–O bond length is essentially constant for all of the phosphine oxide complexes listed in Table 7. A large number of hydrogen-bonded adducts of Ph_3PO have been structurally characterised, but are not considered in the context of this study.[23]

With the exception of the Al–X bonds, the $AlCl_3$ and $AlBr_3$ adducts are structurally indistinguishable. Both structures show relatively short Al–O bonds [X = Cl, O–Al 1.733(4); Br, 1.736(7) Å; *cf.* O–Al single bond 1.78—1.80 Å].[24] Structurally characterised examples of compounds containing a P–O–Al framework are rare.[25] Nevertheless, it is worth noting that the

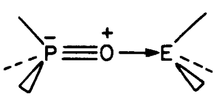
(4)

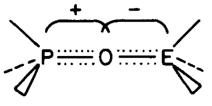
(5)

P–O–Al angles observed in these compounds ($[\{Al(PO_4)(HCl)(EtOH)_4\}_4]$, 146.4, 166.3, and 148.1°;[25a] $(AlMe)(Ph_2COPPh_2)_2(AlMe_2)_2$, <180°;[25b] $(AlCl_3)_2[(Ph_2PO)_2CH_2]$, 164.0°;[25c] $AlPO_4$, 145°[25d]) are significantly less than 180°. [Since the submission of this work the first crystallographic characterisation of Ph_3PO co-ordinated to an aluminium centre has been reported, $Ph_3PO{\cdot}AlO_3(SiPh)_7O_9$, P–O–Al 160.4(3)°[25e]]. The Ga–O bond length [1.818(10) Å] of $Ph_3PO{\cdot}GaCl_3$ is also significantly shorter than the normal range of observed Ga–O single bonds (1.87—2.12 Å).[26] The PPh_3 unit and the acid units of all three structures have slightly distorted tetrahedral local geometries, and the phenyl groups adopt a staggered conformation with the X atoms.

Coaxial (Linear) Co-ordinative Bonding.—The electron-rich elements of the second row (N, O, F) are uniquely multidirectional in their ability to form dative (co-ordinate covalent) bonds, as demonstrated by the variety of bond angles exhibited by oxygen in Table 7. This may be a function of the even distribution of non-bonding electrons about the terminal basic centre, or the ability of these centres to effect coincident σ and π donation. The F_3SN molecule (isoelectronic with R_3PO) forms a co-ordination complex with a number of transition metals of the type $[M(NSF_3)_4(AsF_6)_2]$, in which the angle at the donation centre is approximately linear (*e.g.* Mn–N–S, 161.1(4) and 162.0(3)°.[27] Complexes containing the phosphinimine anion (isoelectronic with R_3PO) display a wide range of M–N–P bond angles and a wide variety of N–M distances, which have been rationalised in terms of the presence or absence of N–M π bonding.[28] Similarly, complex fluoride systems are well known to contain two-co-ordinate fluorine centres with many different geometries.[22] A number of reports have described compounds containing Al–O units with unusually large angles at oxygen. For example, an almost linear Al–O–Al [178.0(3)°] moiety is observed in $Al_2O(C_{10}H_8NO)_4$ with short Al–O bonds [1.676(4) and 1.678(4) Å].[29] While the steric constraints of the chelating ligands may be enforcing linearity for the Al–O–Al connection, the unusual conformation and extremely short Al–O bonds are explained in terms of the involvement of unoccupied *d* orbitals of the aluminium centres in the bonding. The phenolate complexes $[AlMe_2(OC_6H_2Me\text{-}4\text{-}Bu^t_2\text{-}2,6)(PMe_3)]$ [Al–O–C 164.5(4)° and Al–O 1.736(5) Å] and $[AlMeCl_2(OC_6H_2Me\text{-}4\text{-}Bu^t_2\text{-}2,6)]^-$ [Al–O–C 164.0(3)° and Al–O 1.713(4) Å] show similar but less pronounced features.[30] Steric effects are evident in these compounds, and may even be responsible for the slight distortion from linearity. Barron and co-workers[30] have theorised that the unoccupied 3*d* orbitals of aluminium are of too high energy to contribute to the Al–O π bonding, and invoke the use of empty *p* orbitals available on aluminium in the form of Al–X σ* antibonding molecular orbitals to explain C–O–Al linearity and the short Al–O bond in the phenolate complexes.

The donating (co-ordination) abilities of phosphine oxides have been extensively investigated by i.r. spectroscopy and there are a number of structural reports on transition-metal complexes (*e.g.* $Cl_3PO{\cdot}MoCl_5$),[31] Group 15 acid complexes (*e.g.* $Me_3PO{\cdot}SbCl_5$),[32] and a Group 13 acid complex ($Ph_3PO{\cdot}BF_3$).[33] Some of these are listed in Table 7. The results presented above represent the extreme examples of linear co-ordinative bonding by an oxygen centre. The boron analogue $Ph_3PO{\cdot}BF_3$ (and $Ph_3AsO{\cdot}BF_3$) has a familiar bent geometry at oxygen [P–O–B 134.5(2)°].[33] On this basis, we conclude that steric influences are not responsible for the observed linearity, and the rare geometries are a function of the electronic environment of the oxygen centre, under the influence of the acceptor capacities of the acid. Nevertheless, the P–O bond lengths of the Lewis acid adducts of Ph_3PO presented in Table 7 are essentially unaffected (range 1.47—1.53 Å) by the type of acid or the overall molecular geometry of the adduct.

The observed modes of co-ordination may be viewed (in organometallic nomenclature) in terms of σ (linear) or π (bent) complexation: the σ complex involving a non-bonding electron pair on the oxygen centre, and the π complex electrons from the PO π manifold. The majority of Ph_3PO complexes in Table 7 are of the σ-type being linear or towards linear, in contrast to the phosphine sulphide and phosphine selenide complexes which are of the π-type.[16] The short Al–O bonds in the linear adducts indicate the existence of auxiliary bonding as observed for the phenolate complexes (see above). Therefore, we envisage an adduct attachment comprising both σ acceptance and π acceptance by the acid centre, employing either empty σ* *p* orbitals or empty *d* orbitals analogous to the bonding proposed in the siloxanes (N.B. $R_3Si\text{–}O\text{–}SiR_3$ is isoelectronic with the $R_3P\text{–}O\text{–}AlX_3$ unit),[34,35] complexes of the siloxide anions,[36] and the pyrophosphate ions (N.B. $P_2O_7^{4-}$ is isolobal to $R_3PO{\cdot}AlX_3$).[35] Such an arrangement can be represented by electronic model structures **(4)** and **(5)**, implying mutually perpendicular π-delocalised manifolds and maintaining the molecular axial symmetry. Nevertheless, it is evident that the standard simple bonding models do not adequately describe the flexible electronic structure of adducts containing second-row electron-rich elements.

Acknowledgements

We thank the Natural Sciences and Engineering Council of Canada (N. B., T. S. C.), the Donors of the Petroleum Research Fund administered by the American Chemical Society (N. B., R. D. R.), the Killam Foundation (B. W. R.), the US National Science Foundation's Chemical Instrumentation Program (R. D. R.), and Dalhousie University for financial support, and the Atlantic Regional Magnetic Resonance Centre for use of the n.m.r. instrument.

References

1 M. W. Schmidt and M. S. Gordon, *Can. J. Chem.*, 1985, **63**, 1609; *J. Am. Chem. Soc.*, 1985, **107**, 1922; P. Molina, M. Alajarin, C. L. Leonardo, R. M. Claramunt, M. de la Concepcion Foces-Foces, F. H. Cano, J. Catalin, J. L. de Paz, and J. Elguero, *ibid.*, 1989, **111**, 353; W. Kutzelnigg, *Angew. Chem., Int. Ed. Engl.*, 1984, **23**, 272; R. Singleton, *J. Chem. Educ.*, 1973, **50**, 538; A. Streitweiser, A. Rajca, R. S. MacDowell, and R. S. Glaser, *J. Am. Chem. Soc.*, 1987, **109**, 4184.

2 R. Hoffmann, *Angew. Chem., Int. Ed. Engl.*, 1982, **21**, 711; A Haas, *Adv. Inorg. Chem. Radiochem.*, 1984, **28**, 168.

3 See, for example, L. Rodehuser, P. R. Rubini, and J-J. Delpuech, *Inorg. Chem.*, 1977, **16**, 2837.

4 'International Tables for *X*-Ray Crystallography,' Kynoch Press, Birmingham, 1974, vol. 4 (Present distributor: Kluwer Academic Publishers, Dordrecht and Boston).

5 G. M. Sheldrick, SHELX 76, a system of computer programs for *X*-ray structure determination as locally modified, University of Cambridge, 1976.

6 G. M. Sheldrick, SHELXS, in 'Crystallographic Computing 3,' eds. G. M. Sheldrick, C. Kruger, and R. Goddard, Oxford University Press, 1985, pp. 175—189.

7 N. Walker and D. Stuart, *Acta Crystallogr., Sect. A*, 1983, **39**, 158.

8 E. K. Davies, 'The Chemgraf Suite,' Chemical Crystallography Laboratory, Oxford, 1984; C. K. Johnson, ORTEP II, A FORTRAN Thermal Ellipsoid Plot Program for Crystal Structure Illustrations, Report ORNL-5138, Oak Ridge National Laboratory, Tennessee, 1976.

9 See, for example, E. Linder, R. Lehner, and H. Scheer, *Chem. Ber.*, 1967, **100**, 1331; W. v. d. Veer and F. Jellinek, *Recl. Trav. Chim. Pays-Bas*, 1966, 85; M. J. Frazer, W. Gerrard, and R. Twaits, *J. Inorg. Nucl. Chem.*, 1963, **25**, 637; F. A. Cotton, R. D. Barnes, and E. Bannister, *J. Chem. Soc.*, 1960, 2199; S. D. Radosavljevic and D. D. Poleti, *Glas. Hemi. Drus., Beograd*, 1979, **44**, 639; S. Milicev and D. Hadzi, *Inorg. Chim. Acta*, 1977, **21**, 201; M. E. Peach and T. C. Waddington, *J. Chem. Soc.*, 1962, 3450; M. Zackrisson and K. I. Alden, *Acta Chem. Scand.*, 1960, **14**, 994.

10 T. A. Albright, W. J. Freeman, and E. E. Schweizer, *J. Org. Chem.*, 1975, **40**, 3437.

11 T. A. Albright, W. J. Freeman, and E. E. Schweizer, *J. Am. Chem. Soc.*, 1975, **97**, 940.

12 H. Noth and B. Wrackmeyer, 'NMR: Basic Principles and Progress,' vol. 14, eds. P. Diehl, E. Fluck, and R. Kosfeld, Springer, New York, 1978.

13 (*a*) J. J. Delpuech, in 'NMR of Newly Accessible Nuclei,' vol. 2, ed. P. Laszlo, Academic Press, New York, 1983, p. 153; (*b*) J. W. Akitt, in 'Multinuclear NMR,' ed. J. Mason, Plenum, New York, 1987, p. 259.

14 J-J. Delpuech, M. R. Khaddar, A. A. Peguy, and P. R. Rubini, *J. Am. Chem. Soc.*, 1975, **97**, 3373.

15 M. Liang, C. Nicholson, and T. Ashworth, *J. Cryst. Mol. Struct.*, 1975, **5**, 423.

16 N. Burford, B. W. Royan, R. E. v. H. Spence, and R. D. Rogers, *J. Chem. Soc., Dalton Trans.*, in the press.

17 D. E. H. Jones, *J. Chem. Soc., Dalton Trans.*, 1972, 567; R. G. Kidd and D. R. Truax, *J. Am. Chem. Soc.*, 1968, **90**, 6867.

18 J. S. Hartman and G. J. Schrobilgen, *Inorg. Chem.*, 1974, **13**, 874.

19 J. Angenault, J. C. Couturier, and C. Perchard, *J. Inorg. Nucl. Chem.*, 1977, **39**, 369.

20 C. Calvo, *Can. J. Chem.*, 1965, **43**, 1139, 1147.

21 (*a*) G. Ruban and V. Zabel, *Cryst. Struct. Commun.*, 1976, **5**, 671; (*b*) G. Bandoli, G. Bortolozzo, D. A. Clemente, U. Croatto, and C. Panattoni, *J. Chem. Soc. A*, 1970, 2778.

22 See, for example, N. N. Greenwood and A. Earnshaw, 'Chemistry of the Elements,' Pergamon, New York, 1984.

23 See, for example, G. Ferguson, *Z. Kristallogr.*, 1988, **185**, 209; L. Golic and V. Kaucic, *Cryst. Struct. Commun.*, 1976, **5**, 319; P. G. Jones and G. M. Sheldrick, *Acta Crystallogr., Sect. B*, 1978, **34**, 1353.

24 J. L. Atwood and M. J. Zaworotko, *J. Chem. Soc., Chem. Commun.*, 1983, 302.

25 (*a*) J. E. Cassidy, J. A. J. Jarvis, and R. N. Rothon, *J. Chem. Soc., Dalton Trans.*, 1975, 1497; (*b*) G. H. Robinson, B. Lee, W. T. Pennington, and S. A. Sangokoya, *J. Am. Chem. Soc.*, 1988, **110**, 6260; (*c*) S. A. Sangokoya, B. Lee, M. F. Self, W. T. Pennington, and G. H. Robinson, *Polyhedron*, 1989, **8**, 1497; (*d*) R. C. Mooney, *Acta Crystallogr.*, 1956, **9**, 728; (*e*) F. J. Feher, T. A. Budzichowski, and K. J. Weller, *J. Am. Chem. Soc.*, 1989, **111**, 7288.

26 M. J. Zaworotko, R. D. Rogers, and J. L. Atwood, *Organometallics*, 1982, **1**, 1179 and refs. therein.

27 B. Buss, W. Clegg, G. Hartmann, P. G. Jones, R. Mews, M. Noltemeyer, and G. M. Sheldrick, *J. Chem. Soc., Dalton Trans.*, 1981, 61.

28 K. Dehnicke and J. Strahle, *Polyhedron*, 1989, **8**, 707.

29 Y. Kushi and Q. Fernando, *J. Am. Chem. Soc.*, 1970, **92**, 91.

30 M. D. Healy, D. A. Wierda, and A. R. Barron, *Organometallics*, 1988, **7**, 2543.

31 T. Ernst, A. El-Kholi, U. Muller, and K. Dehnicke, *Z. Anorg. Allg. Chem.*, 1988, **566**, 7.

32 C. I. Branden and I. Lindqvist, *Acta Chem. Scand.*, 1963, **17**, 353.

33 N. Burford, R. E. v. H. Spence, A. Linden, and T. S. Cameron, *Acta Crystallogr., Sect. C*, in the press.

34 C. Glidewell and D. C. Liles, *J. Chem. Soc., Chem. Commun.*, 1977, 632.

35 R. Steudel, 'Chemistry of the Non-Metals,' English eds. F. C. Nachod and J. J. Zuckerman, Walter de Gruyter, New York, 1977.

36 See, for example, M. Porchia, N. Brianese, U. Casellato, F. Ossola, G. Rossetto, P. Zanella, and R. Graziani, *J. Chem. Soc., Dalton Trans.*, 1989, 677; E. A. Babaien, D. C. Hrncir, S. G. Bott, and J. L. Atwood, *Inorg. Chem.*, 1986, **25**, 4818.

Received 4*th July* 1989; *Paper* 9/02840D